BIOCHEMISTRY
including biophysical chemistry & molecular biology

Article

pubs.acs.org/biochemistry

OccK Channels from *Pseudomonas aeruginosa* Exhibit Diverse Single-Channel Electrical Signatures but Conserved Anion Selectivity

Jiaming Liu,[†] Elif Eren,[‡] Jagamya Vijayaraghavan,[‡] Belete R. Cheneke,[†] Mridhu Indic,[‡] Bert van den Berg,[‡] and Liviu Movileanu*[,†,§,∥]

[†]Department of Physics, Syracuse University, 201 Physics Building, Syracuse, New York 13244-1130, United States

[‡]Program in Molecular Medicine, University of Massachusetts Medical School, Worcester, Massachusetts 01605, United States

[§]Structural Biology, Biochemistry, and Biophysics Program, Syracuse University, 111 College Place, Syracuse, New York 13244-4100, United States

[∥]Syracuse Biomaterials Institute, Syracuse University, 121 Link Hall, Syracuse, New York 13244, United States

Supporting Information

ABSTRACT: *Pseudomonas aeruginosa* is a Gram-negative bacterium that utilizes substrate-specific outer membrane (OM) proteins for the uptake of small, water-soluble nutrients employed in the growth and function of the cell. In this paper, we present for the first time a comprehensive single-channel examination of seven members of the OM carboxylate channel K (OccK) subfamily. Recent biochemical, functional, and structural characterization of the OccK proteins revealed their common features, such as a closely related, monomeric, 18-stranded β-barrel conformation with a kidney-shaped transmembrane pore and the presence of a basic ladder within the channel lumen. Here, we report that the OccK proteins exhibited fairly distinct unitary conductance values, in a much broader range than previously expected, which includes low (~40−100 pS) and medium (~100−380 pS) conductance. These proteins showed diverse single-channel dynamics of current gating transitions, revealing one-open substate (OccK3), two-open substate (OccK4−OccK6), and three-open substate (OccK1, OccK2, and OccK7) kinetics with functionally distinct conformations. Interestingly, we discovered that anion selectivity is a conserved trait among the members of the OccK subfamily, confirming the presence of a net pool of positively charged residues within their central constriction. Moreover, these results are in accord with an increased specificity and selectivity of these protein channels for negatively charged, carboxylate-containing substrates. Our findings might ignite future functional examinations and full atomistic computational studies for unraveling a mechanistic understanding of the passage of small molecules across the lumen of substrate-specific, β-barrel OM proteins.

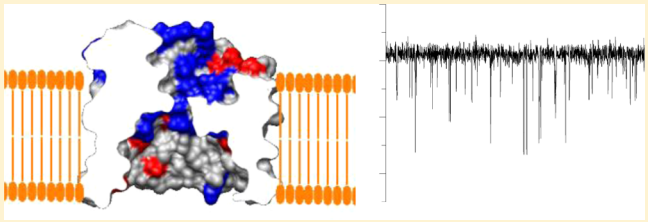

Pseudomonas aeruginosa is a versatile human pathogen that exhibits a fundamental distinction from other Gram-negative organisms such as *Escherichia coli*, its unusually low outer membrane (OM) permeability.[1,2] The major reason for this dissimilarity is the absence of the high-conductance and nonspecific porins, such as OM proteins F (OmpF) and C (OmpC), which are otherwise abundantly present in the OM of *E. coli*. To overcome the poor permeability of their OMs, pseudomonads utilize a range of specialized transport pathways through which the water-soluble, low-molecular mass substrates navigate into the periplasm. OprF is an OM protein A (OmpA) analogue porin in *P. aeruginosa*.[3] It has been shown by single-channel reconstitution into planar lipid bilayers that OprF forms low-conductance protein channels and has an electrical signature decorated by occasional openings.[4] Moreover, *P. aeruginosa* has substrate-specific OM channels, such as OprP[5,6] and OprB,[2,7] which exhibit high transport selectivity for phosphate[3,7] and sugar,[3,7] respectively. The high-resolution X-ray crystal structure of OprP revealed its trimeric assembly, an archetype of the OM porins,[8] and a basic ladder formed by nine arginines that are located from the extracellular surface to the constriction.[9]

However, most small, water-soluble substrates are thought to be taken by the members of the OM carboxylate channel (Occ) family.[2,3,10,11] This OM protein family from *P. aeruginosa* contains 19 substrate-specific channels that share significant amino acid similarity (40−50%).[12] Phylogenetic analysis indicated a division of the Occ family into the OccD and OccK subfamilies.[12,13] The archetypes of these subfamilies are the OccD1[12,14−17] and OccK1[18,19] channels, which are believed to facilitate the uptake of basic amino acids,[12,14,16] and vanillate[13,18] and benzoate,[11] respectively. These sustained efforts to understand the major roles of the proteins of the Occ family were supplemented very recently by Eren and colleagues, who pursued biochemical, functional, and structural analysis of the substrate specificity of three OccD and six OccK protein

Received: January 16, 2012
Revised: February 25, 2012
Published: February 27, 2012

dx.doi.org/10.1021/bi300066w | *Biochemistry* 2012, 51, 2319−2330

channels.[11] This study confirmed that the OccD and OccK proteins share common structural features, such as the monomeric β-barrel conformation, which is quite different from what we have learned previously with trimeric porins of *E. coli*.[20,21] Another hallmark structural trait of the Occ proteins is the presence of a basic ladder of arginines and lysines that are distributed from the extracellular surface to the constriction and from the constriction to the periplasmic surface.[11,17,18]

Therefore, it was proposed that this basic ladder forms an energetically favorable conduit for the small, carboxyl-containing substrates, which are pulled into the cell to sustain its growth and function.[9,11,17,18] The OccK proteins show more variability in terms of shape, size, and charge distribution along the channel longitudinal axis, suggesting distinctions in the functionality within this subfamily.[11] Recent X-ray crystallography information about OccK proteins[11] ignited a detailed biophysical inspection of these subfamily members at the single-channel level. The level of sequence conservation among the residues facing the central constriction of the OccK proteins is generally quite low (Figure S1 of the Supporting Information), so different single-channel electrical signatures were expected.

In this work, we pursued a systematic examination of seven members of the OccK subfamily using single-channel electrophysiology on planar lipid bilayers.[22] The proteins inspected in this work were OccK1−OccK7 (formerly called OpdK, OpdF, OpdO, OpdL, OpdH, OpdQ, and OpdD, respectively). Among these proteins, OccK7 does not have an available crystal structure. Recently, we conducted a detailed biophysical analysis of the OccK1 channel.[19] The results show that all these OccK proteins possess channel forming activity in artificial planar lipid bilayers. We compared the OccK proteins based upon their unitary conductance, their kinetic and energetic data pertinent to single-channel discrete dynamics of their open substates, and their ionic selectivity. None of the OccK proteins forms a high-conductance channel, which is in accord with the recent high-resolution crystallographic information that revealed a narrow central constriction of these channels with a diameter in the range of 3.5−5.0 Å (Figure 1).[11]

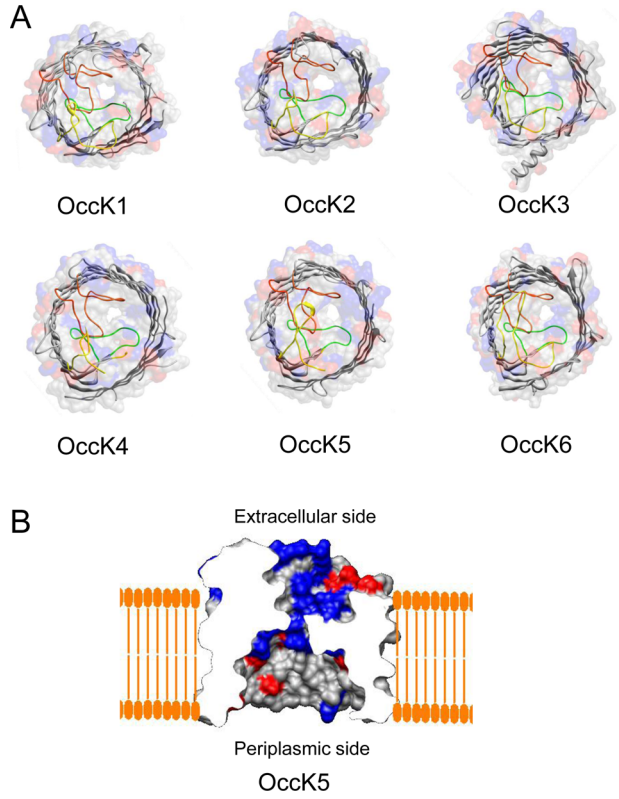

Figure 1. Structural representation of OccK1 family protein channels. (A) Molecular surface and ribbon representations of six OccK subfamily members whose crystal structures have been determined recently,[11] including OccK1−OccK6. On the molecular surface representation, the side chains of positively charged amino acids are colored blue and those of negatively charged amino acids red. On the ribbon representation, constriction-forming loops L3, L4, and L7 are colored green, yellow, and orange, respectively. (B) Side view of the OccK5 channel in a planar lipid bilayer. The charged amino acids are colored as described above. Note the positive surface resulting from the presence of the basic amino acid ladder within the channel constriction.

MATERIALS AND METHODS

Cloning, Expression, and Purification of the OccK Proteins. The mature parts of the *occK* genes from *P. aeruginosa* were amplified by polymerase chain reaction from genomic DNA and cloned into *E. coli* expression vector pB22,[23,24] having the signal sequence of *E. coli* OM protein YtfM and an N-terminal hexahistidine tag for purification. DNA sequencing was performed at the CFAR DNA sequencing facility (UMass Medical School, Worcester, MA). BL21(DE3) T1 phage-resistant cells (New England Biolabs, Ipswich, MA) were transformed with pB22-OccK constructs. The cells were grown to an OD_{600} of 0.6 at 37 °C, induced with 0.1% arabinose at 20 °C overnight, and harvested by centrifugation at 4500 rpm for 30 min (Beckman Coulter, J6-MC). Cell pellets were suspended in TSB [20 mM Tris, 300 mM NaCl, and 10% glycerol (pH 8.0)], and cells were lysed by sonication (3 × 40 s intervals) (Branson Digital Sonifier). Total membranes were obtained by centrifugation at 40000 rpm for 40 min (45 Ti rotor, Beckman L8-70M ultracentrifuge). Membranes were homogenized in TSB and solubilized in 1% DM [*n*-decyl β-D-maltopyranoside (Anatrace, Santa Clara, CA)] and 1% LDAO [*n*-dodecyl-*N*,*N*-dimethylamine *N*-oxide (Anatrace)] for 2 h at 4 °C followed by centrifugation at 40000 rpm for 30 min to remove precipitates and unsolubilized membranes. The membrane extract was applied to a 10 mL nickel column. The column was washed with 10 column volumes (CV) of TSB containing 0.2% DM and 15 mM imidazole. The proteins were eluted with 3 CV of TSB containing 0.2% DM and 200 mM imidazole and further purified by gel filtration chromatography using 10 mM Tris, 50 mM NaCl, and 0.12% DM (pH 8.0). For final polishing and detergent exchange, another gel filtration chromatography step was performed. The buffer used for this column varied depending on the protein; for most of the channels, 10 mM Tris, 50 mM NaCl, and 0.3−0.35% C8E4 were used at pH 8.0. Typically, small amounts (0.02−0.1%) of another detergent (either LDAO, OG, DM, or diheptanoyl-phosphatidylcholine) were added to modify channel solubility. The purified proteins were concentrated to 5−15 mg/mL using 50 kDa molecular mass cutoff filters (Amicon) and directly flash-frozen in liquid nitrogen, without dialysis. The protein samples were aliquoted and kept at −80 °C for several months. The purity of the OccK protein samples was assessed by sodium dodecyl sulfate−polyacrylamide gel electrophoresis.[11]

Single-Channel Current Recordings on Planar Lipid Bilayers. Single-channel current measurements were taken

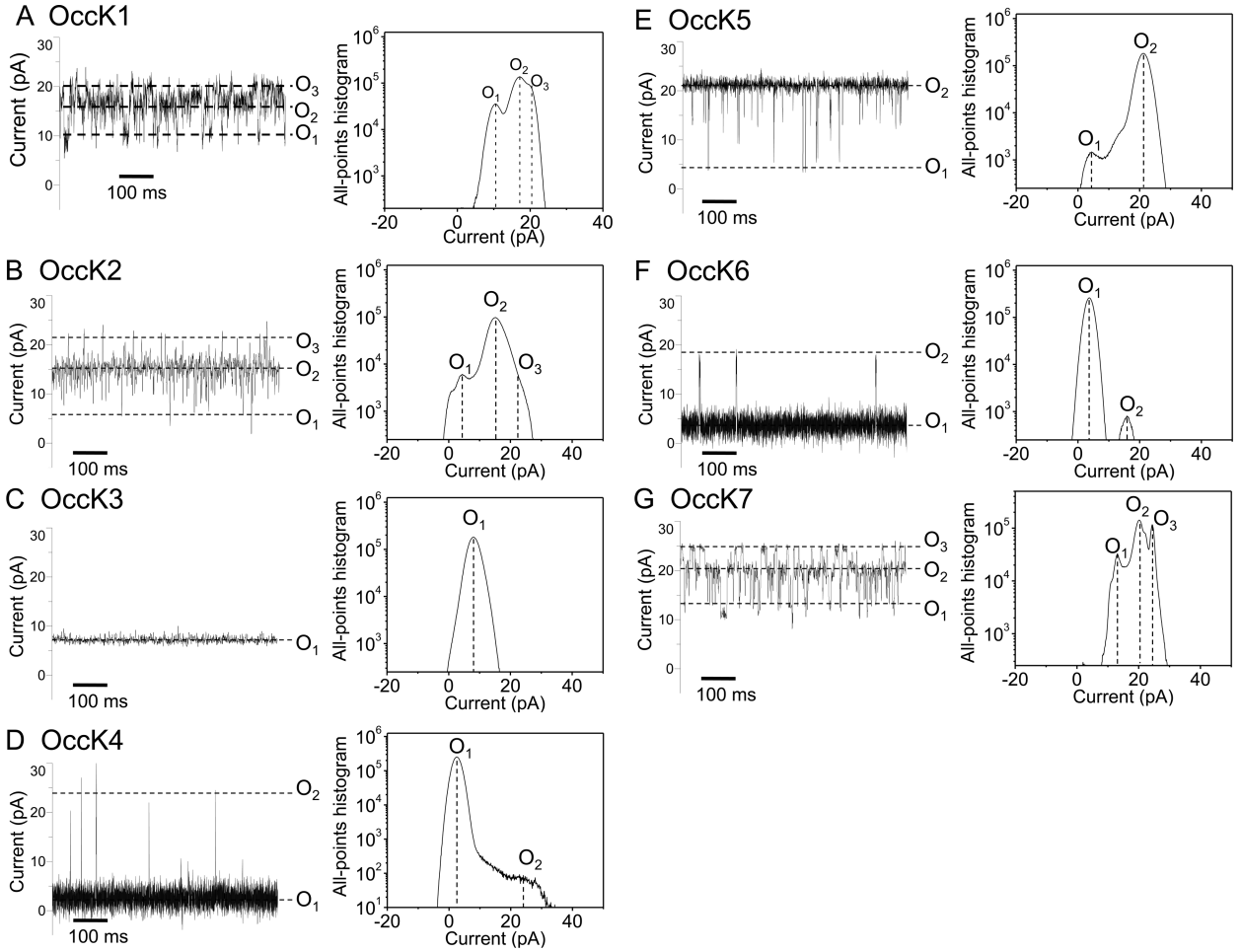

Figure 2. Typical single-channel electrical traces of the OccK subfamily members and the corresponding all-points current amplitude histograms. Traces (left) were recorded at a transmembrane potential of 60 mV in 1 M KCl and 10 mM phosphate (pH 7.4): (A) OccK1, (B) OccK2, (C) OccK3, (D) OccK4, (E) OccK5, (F) OccK6, and (G) OccK7. All-points current amplitude histograms (right) included all acquired data points in a single-channel electrical trace. Current levels were marked on both the single-channel electrical traces and the all-points current amplitude histograms. Substates O_1−O_3 (if applicable) were assigned to the current levels from the lowest to the highest conductance values, respectively. The all-points current amplitude histograms were determined from single experiments, whose electrical traces are shown in the left panels. In this figure, the single-channel electrical traces corresponding to OccK1−OccK3, OccK5, and OccK7 were low-pass Bessel filtered at 2 kHz. Those single-channel electrical traces corresponding to OccK4 and OccK6 were low-pass Bessel filtered at 10 kHz.

with planar lipid membranes.[25,26] Briefly, both chambers (1.5 mL each) of the bilayer apparatus were separated by a 25 μm thick Teflon septum (Goodfellow Corp., Malvern, PA). An aperture in the septum with a diameter of ∼60 μm was pretreated with hexadecane (Aldrich Chemical Co., Milwaukee, WI) dissolved in highly purified *n*-pentane (Burdick & Jackson, Allied Signal Inc., Muskegon, MI) at a concentration of 10% (v/v). The standard electrolyte in both chambers consisted of 1000 mM KCl and 10 mM potassium phosphate (pH 7.4), unless otherwise stated. The bilayer was formed with 1,2-diphytanoyl-*sn*-glycerophosphocholine (Avanti Polar Lipids Inc., Alabaster, AL). OccK proteins were added to the *cis* chamber, which was grounded. A positive current is defined such that it represents a positive charge moving from the *trans* to *cis* chamber. Currents were recorded by using an Axopatch 200B patch-clamp amplifier (Axon Instruments, Foster City, CA) connected to the chambers by Ag/AgCl electrodes. An Optiplex Desktop Computer (Dell, Austin, TX) equipped with a Digitdata 1440 A/D converter (Axon Instruments) was used for data acquisition. The output from this amplifier was also filtered by an eight-pole low-pass Bessel filter (model 900, Frequency Devices, Haverhill, MA) at a frequency of 10 kHz. The sampling rate was 50 kHz. Acquisition and analysis of single-channel data were performed using pClamp version 10.2 (Axon Instruments). The time resolution of the single-channel electrical recordings can be derived using the relationship for the rise time of the filter $T_r = 339/f_c$, where f_c is the corner frequency of the low-pass Bessel filter.[27,28] For example, for an f_c value of 2 kHz, we obtain a T_r of ∼170 μs. This value would give us a dead time (T_d) of $0.54T_r$ = 92 μs. Events shorter than this value were missed. We used protein samples from one or more purification batches and found satisfactory reproducibility of the single-channel electrical signatures. We were able to consistently reproduce the single-channel electrical signatures of 12 members of the Occ family over the past few years.[11,17−19] In this work, all averaged single-channel data resulted from at least three distinct single-channel reconstitutions.

RESULTS

The Members of the OccK Subfamily Feature a Broad Range of Single-Channel Conductance Values. To obtain

dx.doi.org/10.1021/bi300066w | *Biochemistry* 2012, 51, 2319−2330

Table 1. Biophysical Properties of the OccK Proteins[a]

protein	g_{O_1} (pS)[b]	g_{O_2} (pS)[b]	g_{O_3} (pS)[b]	g_{80}/g_{-80}	diameter (Å)	charges located within the constriction
OccK1	223 ± 50	**307 ± 14**	357 ± 24	0.85 ± 0.09	~5.0	(+) R22, R126, R158, R284 (−) D123, D289
OccK2	73 ± 27	**242 ± 40**	371 ± 52	0.77 ± 0.04	~4.5	(+) R26, R129, R161, R280, R327, R387 (−) D126, D292
OccK3	**144 ± 36**	*c*	*c*	0.96 ± 0.26	~3.5	(+) R123, R317, R358, R374 (−) D121, D276, D287
OccK4	**43 ± 11**	358 ± 45	*c*	1.52 ± 0.47	~3.5	(+) R13, R120, R124 (−) D121, D122
OccK5	33 ± 12	**353 ± 22**	*c*	1.28 ± 0.06	~4.0	(+) R31, R134, K179, R334, R374, R376, R392 (−) none
OccK6	**71 ± 34**	302 ± 47	*c*	0.58 ± 0.19	~4.0	(+) R124, R156, R172, R384 (−) D285, E382
OccK7	276 ± 52	**379 ± 45**	463 ± 63	0.98 ± 0.04	*d*	*d*

[a]The single-channel conductance values were measured in 1 M KCl and 10 mM potassium phosphate (pH 7.4). The single-channel conductance that corresponds to the most probable open substate is shown in bold. g_{80}/g_{-80} is the ratio of the conductance of the dominant state at 80 mV to that at −80 mV. The diameters of the OccK proteins in the central constriction were determined using HOLE[59] and their crystal structures.[11] The rightmost column lists the pool of charged residues in the central constriction. This information was obtained by inspecting the lumen of the protein channels using Chimera.[60] [b]The conductance values for these open substates were calculated at a transmembrane potential of 60 mV. [c]This open substate is not present. [d]The crystal structure of the OccK7 protein is not available.

the single-channel electrical characteristics of the OccK proteins, we took our measurements in 1 M KCl and 10 mM potassium phosphate (pH 7.4). The unitary conductance values mentioned below are those corresponding to the most probable open substate of each channel. We determined that the unitary conductance of the OccK proteins covered a broad range, from ~40 to ~380 pS. Here, we define low-, medium-, and high-conductance channels as OM proteins whose single-channel conductances of the most probable open substate are in the ranges of 0−100, 100−500, and 500−1000 pS, respectively. By comparing the unitary conductance among the seven members of the OccK subfamily, we divided them into two groups: (1) the medium-conductance channels, such as OccK1−OccK3, OccK5, and OccK7, whose single-channel conductance values, obtained at 60 mV, were 307 ± 14, 242 ± 40, 144 ± 36, 353 ± 22, and 379 ± 45 pS (n = 3 distinct single-channel experiments), respectively, and (2) the low-conductance channels, which include OccK4 and OccK6, whose single-channel conductance values, under identical conditions, were 43 ± 11 and 71 ± 34 pS (n = 3), respectively.

OccK Proteins Exhibit Multistate, Single-Channel Dynamics. Recently, we showed that OccK1, the archetype of the OccK subfamily, has three major open substates.[19] Figure 2 presents typical single-channel electrical recordings of the seven reconstituted OccK subfamily members, which were collected at a transmembrane potential of 60 mV. Detailed single-channel data analysis permitted direct determination of the current amplitudes of the open substates (Figure 2, the right-hand panels) as well as their average duration (Figure S2 of the Supporting Information).

Interestingly, all OccK proteins, except OccK3, have one dominant (or so-called "most probable") current level, which is decorated by other secondary short-lived open substates. We assigned substates O_1−O_3 (if applicable) to the current levels from the lowest to the highest conductance values, respectively, as marked in Figure 2. Table 1 summarizes the single-channel characteristics of the seven members of the OccK subfamily, including the most probable conductance as well as the channel conductance values associated with each open substate. In addition, Table 1 shows the average diameter and the charged residues of the channel eyelet of the OccK subfamily members. On the basis of the single-channel electrical traces and the all-points current amplitude histograms, we distinguish two groups of channels. The first group includes the three-open substate OccK proteins, such as OccK1 (Figure 2A), OccK2 (Figure 2B), and OccK7 (Figure 2G).[19] These proteins exhibited a most probable open substate O_2, which was decorated by downward current transitions to the low-conductance O_1 open substate and upward current transitions to the high-conductance O_3 open substate. For example, OccK2 showed the most probable O_2 open substate (g_{O_2} = 242 ± 40 pS) that fluctuated between the O_1 open substate (g_{O_1} = 73 ± 27 pS) and the O_3 open substate (g_{O_3} = 371 ± 52 pS). It is also worth mentioning that the OccK proteins that feature this three-open substate kinetics have medium unitary conductance in the range of 240−380 pS.

The second group includes the two-open substate OccK proteins, such as OccK4 (Figure 2D), OccK5 (Figure 2E), and OccK6 (Figure 2F). OccK5 has a dominant O_2 open substate with a relatively high conductance (g_{O_2} = 353 ± 22 pS) and typical gating transitions to the low-conductance O_1 open substate (g_{O_1} = 33 ± 12 pS). Low-conductance protein channels OccK4 and OccK6 exhibited the most probable O_1 open substate, which was accompanied by upward current spikes to the O_2 open substate. Remarkably, the amplitude of the upward current spikes was large, making the single-channel conductance associated with the O_2 open substate (g_{O_2} (OccK4) = 358 ± 45 pS, and g_{O_2} (OccK6) = 302 ± 47 pS) comparable with the conductance range of the medium-conductance OccK proteins, except that of OccK3 (144 ± 36 pS). In contrast to the OccK proteins belonging to these two groups, again OccK3 (Figure 2C) featured only one major open substate (O_1), which was decorated by very low-amplitude and time-irresolvable current fluctuations.

Voltage Dependence of the Unitary Conductance of the OccK Proteins. To better illustrate the multistate behavior, we constructed I−V (current−voltage) profiles for all OccK proteins, revealing the current amplitude of individual open substates at each transmembrane potential examined in

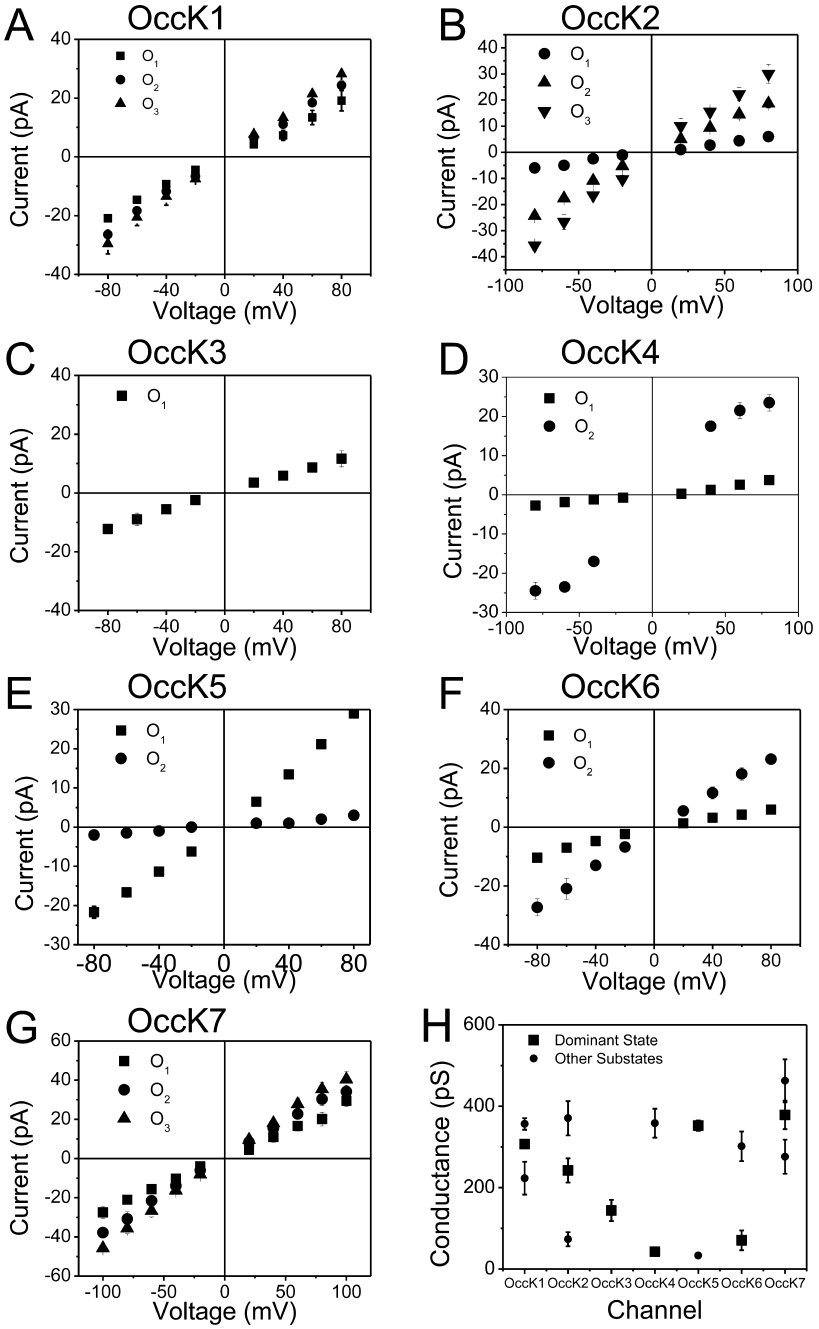

Figure 3. *I*−*V* profiles of all open substates of the OccK subfamily members in 1 M KCl and 10 mM potassium phosphate (pH 7.4): (A) OccK1, (B) OccK2, (C) OccK3, (D) OccK4, (E) OccK5, (F) OccK6, and (G) OccK7. (H) The plots represent the conductance levels of each open substate. The squares indicate the conductance values corresponding to the most probable open substate of each channel. The circles denote the conductance values corresponding to the low-probability open substates of each channel. These conductance values are also listed in Table 1.

this work (Figure 3). The range of the transmembrane potential used here was −80 to 80 mV, because at voltages greater than these some OccK proteins became unstable. The *I*−*V* profiles demonstrate that most of these protein channels exhibited nonohmic voltage dependence. Here, we introduce the asymmetry ratio (g_{80}/g_{-80}). This parameter is defined as the ratio between the unitary conductance at 80 mV and the unitary conductance at −80 mV. The values of g_{80}/g_{-80} are listed in Table 1. All these ratios corresponded to the most probable open substate of each channel. OccK3 and OccK7 showed ohmic voltage dependence of their unitary conductance. In contrast, all other OccK proteins featured asymmetric voltage dependence. The OccK6 channel exhibited the largest asymmetry with a g_{80}/g_{-80} of 0.58 ± 0.19. On the basis of their asymmetry ratio, we found that each channel has a preferred orientation for its insertion into the planar lipid bilayer, because this parameter could be reproduced over ∼80% of the executed single-channel experiments, yet in ∼20% of single-channel experiments, the orientation was flipped, resulting in a reciprocal value of the asymmetry ratio.

Kinetics and Energetics of Current Gating Transitions in OccK Proteins. The current gating transitions in OccK proteins were further examined in detail using standard dwell time histograms (Figure S2 of the Supporting Information).[19]

dx.doi.org/10.1021/bi300066w | *Biochemistry* 2012, 51, 2319−2330

All the dwell time histograms were fit to single-exponential distributions, as judged by log likelihood ratio (LLR) tests with a confidence level of 95%.[29] The fitting results gave us the mean lifetime, which is the reciprocal of the transition rates. For the two-open substate channels (OccK4−OccK6), we employed a simple two-open substate kinetic model, which has two wells and one energetic barrier (Figure 4A):

$$O_1 \leftrightarrow O_2$$

This kinetic scheme has two kinetic rate constants, $k_{O_1 \to O_2}$ and $k_{O_2 \to O_1}$.

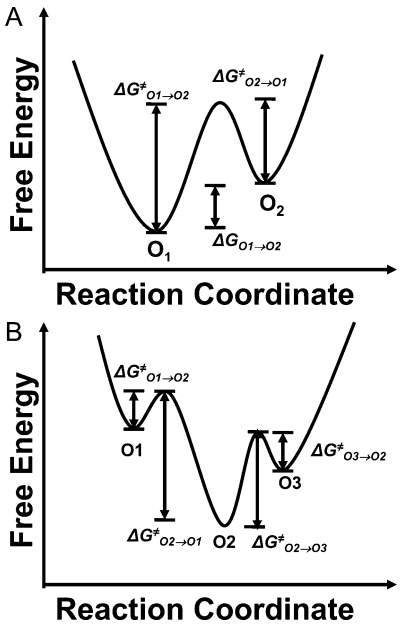

Figure 4. Free energy landscapes of the current gating transitions found in OccK proteins. (A) Free energy landscape for the two-open substate kinetic model, in which the O_1 level is assigned to the most probable open substate. (B) Free energy landscape for the three-open substate kinetic model, in which the O_2 level is assigned to the most probable open substate.

For three-open substate channels (OccK1, OccK2, and OccK7), we constructed a linear model with three wells and two energetic barriers (Figure 4B):

$$O_1 \leftrightarrow O_2 \leftrightarrow O_3$$

This kinetic scheme has four kinetic rate constants: $k_{O_1 \to O_2}$, $k_{O_2 \to O_1}$, $k_{O_3 \to O_2}$, and $k_{O_2 \to O_3}$. The details of this linear kinetic model are described in the Supporting Information. Here, we show the kinetic data of six OccK proteins (Figure 5). In addition to the transition rate constants, we estimated their corresponding activation free energies based on the standard Arrhenius equation:

$$k = \mathrm{ff} \times e^{-\Delta G^{\ddagger}/RT} \quad (1)$$

where k is the kinetic rate constant, ff is the frequency factor, $\Delta G^{\ddagger}$ is the activation free energy, and R and T are the gas constant and absolute temperature, respectively.

The frequency factor in single-channel kinetics is usually taken to be 10^6 s^{-1}.[30] After calculating the activation free energy, we can determine the free energy difference (ΔG°) between two open substates. The free energy difference has a clear physical meaning; i.e., it reflects the probability ratio between different open substates:

$$\Delta G^{\circ}{}_{O_1 \to O_2} = -\ln\left(\frac{k_{O_1 \to O_2}}{k_{O_2 \to O_1}}\right) \quad (2)$$

In Figure 5, we also show the scale of activation free energies. We present the kinetic rate constants on the right y-axis and the corresponding free energy expressed in RT units on the left y-axis to show the voltage dependence of these transitions. Note that as the activation free energy increases the rate constant decreases. The rate constant axis is in a logarithm scale, and the positive direction is downward. We were not able to find a voltage dependence of the kinetic rate constants for protein channels such as OccK2, OccK5, and OccK7. For instance, $k_{O_1 \to O_2}$, $k_{O_2 \to O_1}$, $k_{O_3 \to O_2}$, and $k_{O_2 \to O_3}$ of the OccK2 protein were always in the range of ∼4200 ± 1500, ∼35 ± 15, ∼8000 ± 3000, and ∼15 ± 10 s^{-1}, respectively, regardless of the applied voltage (Figure 5A). Similarly, $k_{O_1 \to O_2}$ and $k_{O_2 \to O_1}$ of the OccK5 protein were always ∼1800 ± 300 and ∼65 ± 15 s^{-1}, respectively (Figure 5C). OccK7 exhibited a similar voltage-independent kinetic profile (Figure 5E). In contrast, the low-conductance OccK4 and OccK6 channels revealed a voltage dependence of their kinetic rate constants and of their free energy difference between the open substates (Figure 5C,E).

Voltage Dependence of the Free Energy Landscapes of the Low-Conductance OccK4 and OccK6 Channels. We constructed the voltage-dependent models of the free energy landscape of the low-conductance OccK protein channels (Figure 6A,B). OccK4 displayed a greater kinetic rate constant from O_1 to O_2 at increased transmembrane potentials. For example, $k_{O_1 \to O_2}$ was 3.2 ± 1.1 and 20.0 ± 8.9 s^{-1} at transmembrane potentials of 40 and 80 mV, respectively. In contrast, $k_{O_2 \to O_1}$ decreased at increasing transmembrane potentials. At 40 mV, $k_{O_2 \to O_1}$ had a value of (16.9 ± 4.1) × 10^3 s^{-1}, whereas at 80 mV, its value was (9.7 ± 0.3) × 10^3 s^{-1}. These results were also obtained at a negative polarity of the applied transmembrane potential, revealing the symmetry of the kinetic transitions in OccK4 with respect to voltage. We conclude that increasing the applied transmembrane potential decreases the activation free energy of the $O_1 \to O_2$ current transitions but increases the activation free energy of the $O_2 \to O_1$ current transitions (Figure 6A). On the other hand, OccK6 showed a monotonic decrease in the $k_{O_1 \to O_2}$ kinetic rate constant from 10.1 ± 1.3 to 2.3 ± 0.3 s^{-1}, when the transmembrane potential increased from −80 to 80 mV, whereas the $k_{O_2 \to O_1}$ kinetic rate constant remained unaltered in the range of ∼650 ± 150 s^{-1}. Therefore, the activation free energy of the $O_1 \to O_2$ current fluctuations increased when the voltage shifted toward more positive values, whereas the activation free energy of the $O_2 \to O_1$ current fluctuations did not undergo a statistically significant alteration (Figure 6B).

Detailed Inspection of the Ion Selectivity of the OccK1 Channel, the Archetype of the OccK Subfamily. We explored the preferential permeability of OccK1 for cations versus anions in the form of permeability ratio (P_K/P_{Cl}). The salt gradient assay was employed to determine the reversal

dx.doi.org/10.1021/bi300066w | Biochemistry 2012, 51, 2319−2330

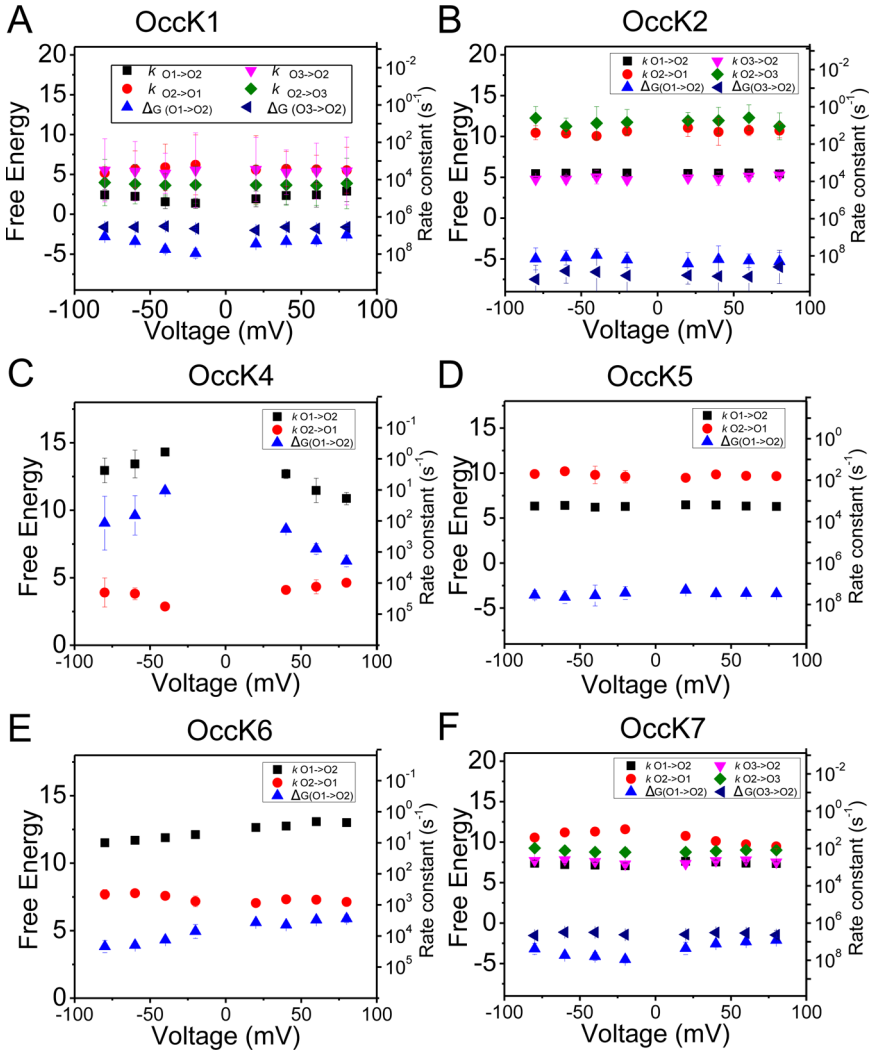

Figure 5. Kinetic rate constants of the current gating transitions and their corresponding free energy differences as well as estimated activation free energies: (A) OccK1, (B) OccK2, (C) OccK4, (D) OccK5, (E) OccK6, and (F) OccK7. The activation free energies were estimated using a frequency factor of 10^{-6} s^{-1}.[30] The left *y*-axes are the free energies in *RT* units, whereas the right *y*-axes are the corresponding kinetic rate constants. Note that the kinetic rate constant axis is in a log scale, and the positive direction is downward.

potential (V_r). The calculation of the permeability ratio was achieved using the Goldman−Hodgkin−Katz formalism:[31,32]

$$\frac{P_K}{P_{Cl}} = \frac{[a_{Cl^-}]_t - [a_{Cl^-}]_c e^{V_r F/RT}}{[a_{K^+}]_t e^{V_r F/RT} - [a_{K^+}]_c} \quad (3)$$

where the variable *a* represents the activity of either potassium or chloride in either the *cis* (subscript *c*) or *trans* (subscript *t*) chamber. Here, *F*, *R*, and *T* are the Faraday constant, the gas constant, and the absolute temperature, respectively.

First, we comprehensively inspected the ion selectivity of the OccK1 channel under various experimental circumstances, including different salt concentration gradients and different pH values. The current−voltage curves, which were determined at asymmetric ionic concentrations, are shown in Figure 7. The *x*-axis intercept of the *I*−*V* curve is the desired reversal potential, which is used to offset the resting potential, making the current zero. In Table 2, we present the reversal potential (V_r) and the calculated P_K/P_{Cl} (eq 3). Here, we define weakly anion selective, anion selective, and strongly anion selective channels as OM proteins whose permeability ratios (P_K/P_{Cl}) are in the ranges of 0.2−1.0 (P_{Cl}/P_K in the range of 1−5), 0.1−0.2 ($P_{Cl}/P_K \approx 5-10$), and 0.01−0.1 ($P_{Cl}/P_K \approx 10-100$), respectively.

Under all asymmetric conditions, the OccK1 protein exhibited a weak anion selectivity. For instance, under the experimental circumstances employed in this work, P_K/P_{Cl} was in the range of 0.35−0.79, so P_{Cl}/P_K was in the range of 1.3−2.9. Parts A and B of Table 2 show the permeability ratios at pH 6.0 and 8.0, respectively, which give no statistically significant differences. The permeability ratios were greater when the KCl concentration was higher in the *cis* chamber than in the *trans* chamber. The reversal potentials were positive when the KCl concentration was higher in the *trans* chamber than in the *cis* chamber. When c_{cis} = 0.2 M KCl and c_{trans} = 1 M KCl, the reversal potentials at pH 6.0 and 8.0 were 13 ± 4 and 16 ± 1 mV (n = 3), respectively. On the other hand, when c_{cis} = 1 M KCl and c_{trans} = 0.2 M KCl, the reversal potentials at pH 6.0 and 8.0 were −3.2 ± 0.4 and −6.4 ± 3.2 mV (n = 3), respectively. Although different salt gradients resulted in slightly different values of selectivity (from ∼0.4 to ∼0.8), all these results hold the sign of the preferred charge; i.e., the OccK1 channel always preferably allows Cl^- to penetrate more than K^+, regardless of the experimental circumstances. The

dx.doi.org/10.1021/bi300066w | *Biochemistry* 2012, 51, 2319−2330

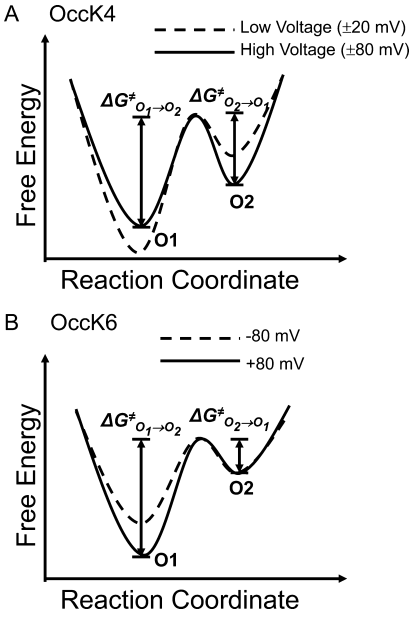

Figure 6. Voltage-dependent free energy landscapes of the low-conductance OccK4 and OccK6 channels. (A) Voltage dependence of the free energy landscape of the OccK4 channel. (B) Voltage dependence of the free energy landscape of the OccK6 channel.

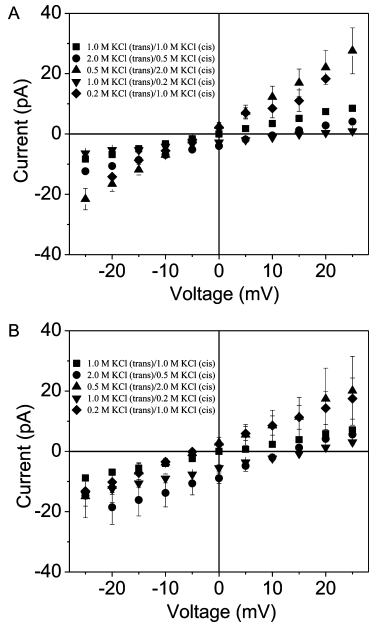

Figure 7. *I*–*V* profiles of the OccK1 channel at asymmetric salt concentrations at (A) pH 6.0 and (B) 8.0. The corresponding numerical results pertinent to the ion selectivity features of OccK1 are listed in Table 2. The buffer solution contained 10 mM potassium phosphate.

weak anion selectivity of the OccK1 channel is likely a result of the basic arginine ladder on the pore walls.[18] This observation is also in accord with the anionic nature of the preferred substrate of this channel (e.g., benzoate).[11]

The Anion Selectivity Is a Conserved Feature in the OccK Subfamily. We also inspected the ion selectivity of all six other OccK channels under one similar experimental condition, i.e., 0.2 M KCl in the *cis* chamber, 1 M KCl in the *trans* chamber, and 10 mM potassium phosphate (pH 7.4). All the results are listed in Table 3. Strikingly, except for OccK3, all OccK proteins were anion selective. OccK5 was strongly anion selective, with P_K/P_{Cl} values of 0.01 ± 0.02. This finding correlated well with the presence of a net pool of seven positively charged residues in the central constriction of the OccK5 channel (Table 1). OccK7 exhibited moderate anion selectivity (P_K/P_{Cl} = 0.18 ± 0.02), whereas OccK1, OccK2, OccK4, and OccK6 were weakly anion selective, with P_K/P_{Cl} ranging from ∼0.3 to ∼0.7. Overall, these results are in line with the net negative pool of positively charged residues in the central eyelet of the channel.

Table 2. Permeability Ratios and Reversal Potentials Determined for the OccK1 Protein under Various Experimental Conditions at (A) pH 6.0 and (B) 8.0[a]

cis c_{KCl} (M)	*trans* c_{KCl} (M)	V_r (mV)	P_K/P_{Cl}
	(A)		
1	0.2	−3.2 ± 0.4	0.79 ± 0.04
0.2	1	13 ± 4	0.38 ± 0.07
2	0.5	−3.1 ± 0.6	0.77 ± 0.06
0.5	2	12.1 ± 0.6	0.48 ± 0.08
	(B)		
1	0.2	−6.4 ± 3.2	0.66 ± 0.12
0.2	1	15.9 ± 1.3	0.35 ± 0.03
2	0.5	−3.8 ± 0.6	0.79 ± 0.03
0.5	2	14.1 ± 2.0	0.36 ± 0.05

[a]The single-channel data were obtained under asymmetric conditions. The permeability ratio P_K/P_{Cl} was calculated using reversal potential (V_r). The buffer solutions contained 10 mM potassium phosphate. The data represent averages ± standard deviations over a number of at least three distinct single-channel recordings.

Table 3. Ion Selectivities of the OccK Proteins[a]

protein	V_r (mV)	P_K/P_{Cl}	selectivity
OccK1	15.9 ± 1.3	0.35 ± 0.03	weakly anion selective channel
OccK2	7.9 ± 1.0	0.63 ± 0.04	weakly anion selective channel
OccK3	∼0	∼1	nonselective channel
OccK4	13.3 ± 1.5	0.45 ± 0.04	weakly anion selective channel
OccK5	42.7 ± 3.1	∼0.01 ± 0.02	strongly anion selective channel
OccK6	6.7 ± 2.5	0.68 ± 0.10	weakly anion selective channel
OccK7	25.7 ± 1.5	0.18 ± 0.02	anion selective channel

[a]The reversal potential (V_r) is the applied transmembrane potential that offsets the resting potential of the channel in a 0.2 M KCl salt gradient on the *cis* side and a 1 M KCl salt gradient on the *trans* side. The chamber also contained 10 mM potassium phosphate (pH 7.4). The reversal potentials (V_r) were provided as averages ± the standard deviation over at least three independent single-channel experiments.

DISCUSSION

In this work, we conducted an extensive single-channel examination of the members of the OccK subfamily from *P. aeruginosa*. This detailed study was prompted by recent biochemical, functional, and structural analysis of the substrate specificity among the outer membrane carboxylate channels (Occ).[11] These OM protein channels exhibited diverse single-channel electrical signatures, including a broad range of unitary conductance, between 40 and 380 pS, a wide variety of transient current gating fluctuations, departing from the most probable open substate to other secondary open substates of shorter duration, and a spectrum of non-ohmic voltage dependence of their conductance. The OccK subfamily proteins

dx.doi.org/10.1021/bi300066w | *Biochemistry* 2012, 51, 2319−2330

displayed low- and medium-conductance open substates. For example, in the case of OccK1, OccK2, OccK5, and OccK7, the channel mostly remained on the medium-conductance O_2 open substate (240−380 pS), from which either reversible fluctuations toward the low-conductance O_1 open substate (OccK5) or multiple current transitions comprising a low-conductance O_1 open substate and a medium-conductance O_3 open substate (OccK1, OccK2, and OccK7) were observed.

For the three-open substate channels, we were not able to find direct transitions between the O_1 and O_3 open substates, suggesting that the $O_1 \leftrightarrow O_2$ and $O_2 \leftrightarrow O_3$ current transitions were made by distinct parts of the protein that fluctuated independently of each other. Another common feature among this group of channels is the fact that the $O_2 \leftrightarrow O_3$ current transitions occurred with a greater kinetic rate constant than the $O_1 \leftrightarrow O_2$ current transitions. Moreover, in OccK1,[19] OccK2, and OccK7 channels, the high-frequency $O_2 \leftrightarrow O_3$ current transitions displayed a current amplitude lower than the value corresponding to the low-frequency $O_1 \leftrightarrow O_2$ current transitions (Figures 2−4). These striking similarities in the current amplitudes and event frequencies of the gating transitions observed in this work indicate that OccK1, OccK2, and OccK7 have similar mechanisms for the discrete current transitions among open substates O_1−O_3.

In contrast, low-conductance OccK4 and OccK6 proteins dwelled for long periods of time on the low-conductance O_1 open substate (40−70 pS) and fluctuated in the form of infrequent and short-lived upward current transitions to a medium-conductance O_2 open substate (302−358 pS). However, one distinction between the OccK4 and OccK6 protein channels is the voltage dependence of their current transitions (Figure 6). This finding suggests that different mechanisms of the fluctuating parts of the low-conductance OccK channels are involved, resulting in upward large-amplitude current spikes that produce a more permeable pore. The members of the Occ family feature ∼40−50% sequence similarity, and the OccK subfamily members share an even greater sequence similarity of ∼50−55% (Figure S1 of the Supporting Information).[3,7,11] According to the recently determined, high-resolution crystal structures of the OccK proteins, the diameter of their constriction, including the molecular surface generated by the van der Waals radii, varies in a narrow range, from ∼3.5 to ∼5 Å (Table 1). On the other hand, the X-ray crystal structures of the OccK proteins were determined at widely varying pH values, between pH 4 and 8.5.[11]

The unitary conductance should be a complex function that depends not only on the cross-sectional diameter of the central constriction but also on the average diameter along the longitudinal axis along the channel lumen, and the charge distribution throughout the inner surface of the protein. The most probable open substate in the OccK protein depends on the orientation of large extracellular loops L3, L4, and L7 within the pore lumen. The single-channel electrical signatures of these OccK proteins are highly diverse (Figure 2), suggesting that, despite their sequence homology and closely similar cross-sectional diameter of the central constriction, minor alterations in the length, packing, and structure of the extracellular loops located within the channel lumen (Figure S2 of the Supporting Information) have drastic implications on the unitary conductance as well as the functionality of these proteins.[33,34]

Several experimental details of our single-channel electrical recordings, such as the lipid composition of the membranes, the applied transmembrane potential, and the ion concentration in the chamber, depart from the physiological environment of *P. aeruginosa*.[2,35] Given the duration of the fast and transient current fluctuations, it is conceivable that the single-channel current measured with the members of the OccK subfamily in 150 mM KCl at a transmembrane potential that is specific to outer membrane proteins (approximately several millivolts) would not allow the detection of resolvable open substates. Therefore, a meaningful comparison among all members of the OccK subfamily required a substantial improvement in the signal-to-noise ratio, which was accomplished by using a buffer solution containing 1 M KCl and greater transmembrane potential values. One concern of using a higher salt concentration is the alteration of the substate dynamics. In a recent work, the change in salt concentration had a substantial impact on the single-channel electrical signature of the staphylococcal α-hemolysin.[36] However, for the OccK1 protein, we performed single-channel electrical recordings using 500 mM KCl in the chamber, which is much closer to the physiological condition. In this case, we observed a conserved number of open substates (O_1−O_3).[19]

Interestingly, we found that the OccK proteins are anion selective, a feature conserved among members of this subfamily. Our investigations also show a detailed analysis of the selectivity measurements of the OccK1 channel, which were performed under different KCl gradient and pH conditions. We were not able to find an impact of pH, in the range of pH 6−8, on the ionic selectivity of the OccK1 channel. This result suggests a lack of chargeable groups within the channel lumen under these conditions. Indeed, a careful inspection of the X-ray crystal structure of this channel revealed that histidine residues (pK_a = 6) are located outside the channel lumen. The highly conserved anion selectivity among the members of the OccK subfamily in *P. aeruginosa* is in accord with the net pool of positively charged residues, such as arginines and lysines, in the central constriction of the channel (Table 1 and Figure S1 of the Supporting Information). The OccK proteins, whose crystal structure are available, show either one (OccK3 and OccK4), two (OccK1 and OccK6), four (OccK2), or seven (OccK5) net positive charges in the channel eyelet. In agreement with these structural distinctions among the members of the OccK subfamily, we determined that OccK5 is a strongly anion selective channel (Table 3). This correlation also holds for OccK3 and OccK4, which are nonselective and poorly anion selective channels, respectively. These ion selectivity results are also compatible with the substrate specificity of members of the OccK subfamily. For example, carboxylate-containing benzoate, gluconorate, and pyroglutamate are the preferred substrates for OccK1−OccK3, respectively.[11] On the other hand, members of the OccD subfamily do not transport these molecules. Most of the OccD channels transport arginine very well. Shall we anticipate that the OccD subfamily members are cation selective? If this is true, then this difference in ion selectivity among the members of the OccK and OccD subfamilies will add to the already known structural, phylogenetic, and functional distinctions.

The positively charged residues within the central constriction of the OccK proteins might function as catalyzers for the passage of carboxylate-containing substrates across the channel lumen. This mechanism is also present in other substrate-specific outer membrane proteins, such as the maltoporin of *E. coli*, which represents the pathway for sugar uptake. In this case, the attractive sites are aromatic residues,

thus reducing the activation free energies for the translocation of sugar from one side of the membrane to the other.[37] In the past, we also demonstrated that attractive sites present within the channel lumen have major implications even for larger molecules, such as polypeptides traversing the channel,[29,38] which is in accord with the theoretical predictions.[39−42]

One question that emerges from this work is how the OccK channels compare with other well-studied substrate-specific or nonspecific outer membrane porins. The medium-conductance OccK channels have a greater conductance than the sugar-specific LamB porin from *E. coli*.[20] LamB features a single-channel conductance of ∼53 pS per each monomer in 1 KCl.[43] This value is comparable with the single-channel conductance of the low-conductance OccK4 (∼43 pS) and OccK6 (∼71 pS) channels. This work also confirms that the OccK channels show a unitary conductance that is smaller than the value corresponding to nonspecific outer membrane porins from *E. coli*, such as the trimeric OmpF (∼700 pS per monomer in 1 M KCl[44,45]) and OmpC (∼900 pS per monomer in 1 M KCl[46]) channels. Each monomer of these outer membrane proteins forms a 16-stranded β-barrel with a central constriction made by the inwardly folded L3 extracellular loop.[47]

How do the OccK and OccD subfamily members compare to each other? Recent work performed by our teams demonstrated that the observed most probable conductance values of the OccD and OccK subfamily members are generally in accord with the available crystal structures.[11] For instance, the most probable conductance of OccD1 and OccD2 is ∼20 pS, which is very consistent with the very small diameter of these channels (<3 Å).[17] These results are also in accordance with prior electrophysiological studies performed by Ishii and Nakae, who discovered a very small unitary conductance (∼30 pS) in recordings with the OccD1 channel.[48,49] The OccK subfamily includes a channel, OccK4, that also exhibits a very low conductance [∼43 pS (Table 1)]. However, we determined that the most probable unitary conductance of the OccD3 channel is ∼700 pS, the largest value among all examined OccD and OccK channels.[11] This observation is not compatible with the small diameter of the channel eyelet of the OccD3 protein. Obviously, the length, conformation, and location of each extracellular loop impact the single-channel conductance in a similar way in which a water-soluble polymer blocks the ionic flow.[50,51] Huang and Hancock[52] found that a deletion in loop L5 of the OccD1 channel produced a 33-fold increase in single-channel conductance.

Very interestingly, Ishii and Nakae[49] discovered that the OccD1 channel, the archetype of the OccD subfamily in *P. aeruginosa*, exhibited highly frequent, medium-conductance (∼400 pS in 1 M KCl) openings in lipopolysacharide (LPS)-containing lipid bilayers. In LPS-free lipid bilayers, OccD1 showed a low conductance (30 pS). However, in the LPS-containing lipid bilayers, the channel fluctuated between low- (∼30 pS) and medium-conductance (∼400 pS) open substates. Therefore, the lipid environment influenced the functional features of the OccD1 channel. This finding represents strong evidence that the composition of the lipid bilayer impacts the discrete dynamics of the open substates of the OccD1 channel. We speculate that LPS-containing bilayers might be an energetically favorable environment for transient openings of the Occ channels, promoting the transport of specific substrates or even antibiotics.

Molecular dynamics (MD) simulations show a great promise in obtaining a qualitative understanding of the stochastic motions of the extracellular long loops folded back into the channel lumen.[53,54] For example, Bond and colleagues[55] employed MD simulations to study the conformations of the extracellular loops in the outer membrane protein OpcA from *Neisseria meningitidis*. They found that the lipid bilayer environment and physiological salt concentrations affected the conformation of the extracellular loops in OpcA. Therefore, it is conceivable that different crystallization conditions might influence the orientation of the extracellular loops folding back into the channel interior. Moreover, this experimental work might ignite future full-atomistic computational biophysics studies aimed at obtaining a clarification on how small molecules, such as substrates and antibiotics, traverse the complex environment of the channel lumen of members of the OccK subfamily.[56−58]

In summary, we show a detailed high-resolution, single-channel analysis of seven members of the OccK subfamily from *P. aeruginosa*. The electrical signature of the OccK proteins revealed diverse unitary conductance values with well-defined single-channel discrete dynamics, which is comprised of low- and medium-conductance open substates. The current gating transitions among various open substates were likely produced by stochastic fluctuations of the long extracellular loops folded back into the channel lumen. We found that the OccK proteins are anion selective, a feature that is explained at least in part by the presence of the basic ladder of arginine and lysine residues near the central constriction, and that is in accord with structural and in vitro substrate transport reconstitution studies.

■ ASSOCIATED CONTENT

Supporting Information

Amino acid sequence analysis of seven OccK subfamily members, analysis of the single-channel open substate transitions of the OccK proteins, a three-substate kinetic model for the current fluctuations in the OccK proteins, and the standard free energies corresponding to various gating transitions in the OccK1 protein. This material is available free of charge via the Internet at http://pubs.acs.org.

■ AUTHOR INFORMATION

Corresponding Author

*Department of Physics, Syracuse University, 201 Physics Building, Syracuse, NY 13244-1130. Phone: (315) 443-8078. Fax: (315) 443-9103. E-mail: lmovilea@physics.syr.edu.

Funding

This work was funded in part by grants from the National Science Foundation (DMR-1006332 to L.M.) and the National Institutes of Health (R01 GM088403 to L.M. and R01 GM085785 to B.v.d.B.).

Notes

The authors declare no competing financial interest.

■ ACKNOWLEDGMENTS

We thank colleagues in the Movileanu and van den Berg research groups, who provided technical assistance at various stages of this work.

■ ABBREVIATIONS

LamB, sugar-specific porin of *E. coli*; MD, molecular dynamics; OM, outer membrane of Gram-negative bacteria; Occ, outer membrane carboxylate channel family of *P. aeruginosa*; OccD, outer membrane carboxylate channel D subfamily of *P.*

aeruginosa; OccK, outer membrane carboxylate channel K subfamily of *P. aeruginosa*; OmpC, outer membrane protein C of *E. coli*; OmpF, outer membrane protein F of *E. coli*; OprF, outer membrane protein A analogue porin of *P. aeruginosa*.

REFERENCES

(1) Nikaido, H., Nikaido, K., and Harayama, S. (1991) Identification and characterization of porins in *Pseudomonas aeruginosa*. *J. Biol. Chem. 266*, 770−779.

(2) Nikaido, H. (2003) Molecular basis of bacterial outer membrane permeability revisited. *Microbiol. Mol. Biol. Rev. 67*, 593−656.

(3) Hancock, R. E., and Brinkman, F. S. (2002) Function of *Pseudomonas* porins in uptake and efflux. *Annu. Rev. Microbiol. 56*, 17−38.

(4) Nestorovich, E. M., Sugawara, E., Nikaido, H., and Bezrukov, S. M. (2006) *Pseudomonas aeruginosa* porin OprF: Properties of the channel. *J. Biol. Chem. 281*, 16230−16237.

(5) Benz, R., and Hancock, R. E. (1987) Mechanism of ion transport through the anion-selective channel of the *Pseudomonas aeruginosa* outer membrane. *J. Gen. Physiol. 89*, 275−295.

(6) Sukhan, A., and Hancock, R. E. (1996) The role of specific lysine residues in the passage of anions through the *Pseudomonas aeruginosa* porin OprP. *J. Biol. Chem. 271*, 21239−21242.

(7) Hancock, R. E. W., and Tamber, S. (2004) Porins of the Outer Membrane of *Pseudomonas aeruginosa*. In *Bacterial and Eukaryotic Porins: Structure, Function, Mechanism* (Benz, R., Ed.) pp 61−77, Wiley-VCH, Weinheim, Germany.

(8) Schirmer, T. (1998) General and specific porins from bacterial outer membranes. *J. Struct. Biol. 121*, 101−109.

(9) Moraes, T. F., Bains, M., Hancock, R. E., and Strynadka, N. C. (2007) An arginine ladder in OprP mediates phosphate-specific transfer across the outer membrane. *Nat. Struct. Mol. Biol. 14*, 85−87.

(10) Sampathkumar, P., Lu, F., Zhao, X., Li, Z., Gilmore, J., Bain, K., Rutter, M. E., Gheyi, T., Schwinn, K. D., Bonanno, J. B., Pieper, U., Fajardo, J. E., Fiser, A., Almo, S. C., Swaminathan, S., Chance, M. R., Baker, D., Atwell, S., Thompson, D. A., Emtage, J. S., Wasserman, S. R., Sali, A., Sauder, J. M., and Burley, S. K. (2010) Structure of a putative BenF-like porin from *Pseudomonas fluorescens* Pf-5 at 2.6 Å resolution. *Proteins 78*, 3056−3062.

(11) Eren, E., Vijayaraghavan, J., Liu, J., Cheneke, B. R., Touw, D. S., Lepore, B. W., Indic, M., Movileanu, L., and van den Berg, B. (2012) Substrate specificity within a family of outer membrane carboxylate channels. *PLoS Biol. 10*, e1001242.

(12) Tamber, S., and Hancock, R. E. (2006) Involvement of two related porins, OprD and OpdP, in the uptake of arginine by *Pseudomonas aeruginosa*. *FEMS Microbiol. Lett. 260*, 23−29.

(13) Tamber, S., Ochs, M. M., and Hancock, R. E. (2006) Role of the novel OprD family of porins in nutrient uptake in *Pseudomonas aeruginosa*. *J. Bacteriol. 188*, 45−54.

(14) Ochs, M. M., Lu, C. D., Hancock, R. E., and Abdelal, A. T. (1999) Amino acid-mediated induction of the basic amino acid-specific outer membrane porin OprD from *Pseudomonas aeruginosa*. *J. Bacteriol. 181*, 5426−5432.

(15) Ochs, M. M., McCusker, M. P., Bains, M., and Hancock, R. E. (1999) Negative regulation of the *Pseudomonas aeruginosa* outer membrane porin OprD selective for imipenem and basic amino acids. *Antimicrob. Agents Chemother. 43*, 1085−1090.

(16) Trias, J., and Nikaido, H. (1990) Protein D2 channel of the *Pseudomonas aeruginosa* outer membrane has a binding site for basic amino acids and peptides. *J. Biol. Chem. 265*, 15680−15684.

(17) Biswas, S., Mohammad, M. M., Patel, D. R., Movileanu, L., and van den Berg, B. (2007) Structural insight into OprD substrate specificity. *Nat. Struct. Mol. Biol. 14*, 1108−1109.

(18) Biswas, S., Mohammad, M. M., Movileanu, L., and van den Berg, B. (2008) Crystal structure of the outer membrane protein OpdK from *Pseudomonas aeruginosa*. *Structure 16*, 1027−1035.

(19) Cheneke, B. R., van den Berg, B., and Movileanu, L. (2011) Analysis of gating transitions among the three major open states of the OpdK channel. *Biochemistry 50*, 4987−4997.

(20) Schirmer, T., Keller, T. A., Wang, Y. F., and Rosenbusch, J. P. (1995) Structural basis for sugar translocation through maltoporin channels at 3.1 Å resolution. *Science 267*, 512−514.

(21) Yamashita, E., Zhalnina, M. V., Zakharov, S. D., Sharma, O., and Cramer, W. A. (2008) Crystal structures of the OmpF porin: Function in a colicin translocon. *EMBO J. 27*, 2171−2180.

(22) Sackmann, B., and Neher, E. (1995) *Single-Channel Recording*, Kluwer Academic/Plenum Publishers, New York.

(23) Guzman, L. M., Belin, D., Carson, M. J., and Beckwith, J. (1995) Tight regulation, modulation, and high-level expression by vectors containing the arabinose PBAD promotor. *J. Bacteriol. 177*, 4121−4130.

(24) van den, B. B., Clemons, W. M. Jr., Collinson, I., Modis, Y., Hartmann, E., Harrison, S. C., and Rapoport, T. A. (2004) X-ray structure of a protein-conducting channel. *Nature 427*, 36−44.

(25) Howorka, S., Movileanu, L., Lu, X. F., Magnon, M., Cheley, S., Braha, O., and Bayley, H. (2000) A protein pore with a single polymer chain tethered within the lumen. *J. Am. Chem. Soc. 122*, 2411−2416.

(26) Goodrich, C. P., Kirmizialtin, S., Huyghues-Despointes, B. M., Zhu, A. P., Scholtz, J. M., Makarov, D. E., and Movileanu, L. (2007) Single-molecule electrophoresis of β-hairpin peptides by electrical recordings and Langevin dynamics simulations. *J. Phys. Chem. B 111*, 3332−3335.

(27) Colquhoun, D., and Sigworth, F. J. (1995) Fitting and statistical analysis of single-channel records. In *Single-channel recording* (Sackmann, B. N. E., Ed.) 2nd ed., pp 483−587, Plenum Press, New York.

(28) Movileanu, L., Cheley, S., and Bayley, H. (2003) Partitioning of individual flexible polymers into a nanoscopic protein pore. *Biophys. J. 85*, 897−910.

(29) Mohammad, M. M., and Movileanu, L. (2008) Excursion of a single polypeptide into a protein pore: Simple physics, but complicated biology. *Eur. Biophys. J. 37*, 913−925.

(30) Yang, W. Y., and Gruebele, M. (2003) Folding at the speed limit. *Nature 423*, 193−197.

(31) Hille, B. (2001) *Ion Channels of Excitable Membranes*, Sinauer Associates, Inc., Sunderland, MA.

(32) Wolfe, A. J., Mohammad, M. M., Cheley, S., Bayley, H., and Movileanu, L. (2007) Catalyzing the translocation of polypeptides through attractive interactions. *J. Am. Chem. Soc. 129*, 14034−14041.

(33) Jung, Y., Bayley, H., and Movileanu, L. (2006) Temperature-responsive protein pores. *J. Am. Chem. Soc. 128*, 15332−15340.

(34) Mohammad, M. M., Howard, K. R., and Movileanu, L. (2011) Redesign of a plugged β-barrel membrane protein. *J. Biol. Chem. 286*, 8000−8013.

(35) Sen, K., Hellman, J., and Nikaido, H. (1988) Porin channels in intact cells of *Escherichia coli* are not affected by Donnan potentials across the outer membrane. *J. Biol. Chem. 263*, 1182−1187.

(36) Mohammad, M. M., and Movileanu, L. (2010) Impact of distant charge reversals within a robust β-barrel protein pore. *J. Phys. Chem. B 114*, 8750−8759.

(37) Hilty, C., and Winterhalter, M. (2001) Facilitated substrate transport through membrane proteins. *Phys. Rev. Lett. 86*, 5624−5627.

(38) Bikwemu, R., Wolfe, A. J., Xing, X., and Movileanu, L. (2010) Facilitated translocation of polypeptides through a single nanopore. *J. Phys.: Condens. Matter 22*, 454117.

(39) Berezhkovskii, A. M., Pustovoit, M. A., and Bezrukov, S. M. (2002) Channel-facilitated membrane transport: Transit probability and interaction with the channel. *J. Chem. Phys. 116*, 9952−9956.

(40) Berezhkovskii, A. M., and Bezrukov, S. M. (2005) Optimizing transport of metabolites through large channels: Molecular sieves with and without binding. *Biophys. J. 88*, L17−L19.

(41) Kolomeisky, A. B., and Kotsev, S. (2008) Effect of interactions on molecular fluxes and fluctuations in the transport across membrane channels. *J. Chem. Phys. 128*, 085101.

(42) Bauer, W. R., and Nadler, W. (2006) Molecular transport through channels and pores: Effects of in-channel interactions and blocking. *Proc. Natl. Acad. Sci. U.S.A. 103*, 11446−11451.
(43) Benz, R., Schmid, A., Nakae, T., and Vos-Scheperkeuter, G. H. (1986) Pore formation by LamB of *Escherichia coli* in lipid bilayer membranes. *J. Bacteriol. 165*, 978−986.
(44) Saint, N., Lou, K. L., Widmer, C., Luckey, M., Schirmer, T., and Rosenbusch, J. P. (1996) Structural and functional characterization of OmpF porin mutants selected for larger pore size. II. Functional characterization. *J. Biol. Chem. 271*, 20676−20680.
(45) Chimerel, C., Movileanu, L., Pezeshki, S., Winterhalter, M., and Kleinekathofer, U. (2008) Transport at the nanoscale: Temperature dependance of ion conductance. *Eur. Biophys. J. 38*, 121−125.
(46) Biro, I., Pezeshki, S., Weingart, H., Winterhalter, M., and Kleinekathofer, U. (2010) Comparing the temperature-dependent conductance of the two structurally similar *E. coli* porins OmpC and OmpF. *Biophys. J. 98*, 1830−1839.
(47) Cowan, S. W., Garavito, R. M., Jansonius, J. N., Jenkins, J. A., Karlsson, R., Konig, N., Pai, E. F., Pauptit, R. A., Rizkallah, P. J., and Rosenbusch, J. P. (1995) The structure of OmpF porin in a tetragonal crystal form. *Structure 3*, 1041−1050.
(48) Ishii, J., and Nakae, T. (1996) Specific interaction of the protein-D2 porin of *Pseudomonas aeruginosa* with antibiotics. *FEMS Microbiol. Lett. 136*, 85−90.
(49) Ishii, J., and Nakae, T. (1993) Lipopolysaccharide promoted opening of the porin channel. *FEBS Lett. 320*, 251−255.
(50) Movileanu, L., and Bayley, H. (2001) Partitioning of a polymer into a nanoscopic protein pore obeys a simple scaling law. *Proc. Natl. Acad. Sci. U.S.A. 98*, 10137−10141.
(51) Movileanu, L., Cheley, S., Howorka, S., Braha, O., and Bayley, H. (2001) Location of a constriction in the lumen of a transmembrane pore by targeted covalent attachment of polymer molecules. *J. Gen. Physiol. 117*, 239−251.
(52) Huang, H., and Hancock, R. E. (1996) The role of specific surface loop regions in determining the function of the imipenem-specific pore protein OprD of *Pseudomonas aeruginosa*. *J. Bacteriol. 178*, 3085−3090.
(53) Luan, B., Caffrey, M., and Aksimentiev, A. (2007) Structure refinement of the OpcA adhesin using molecular dynamics. *Biophys. J. 93*, 3058−3069.
(54) Luan, B., Carr, R., Caffrey, M., and Aksimentiev, A. (2010) The effect of calcium on the conformation of cobalamin transporter BtuB. *Proteins 78*, 1153−1162.
(55) Bond, P. J., Derrick, J. P., and Sansom, M. S. (2007) Membrane simulations of OpcA: Gating in the loops? *Biophys. J. 92*, L23−L25.
(56) Hajjar, E., Bessonov, A., Molitor, A., Kumar, A., Mahendran, K. R., Winterhalter, M., Pages, J. M., Ruggerone, P., and Ceccarelli, M. (2010) Toward screening for antibiotics with enhanced permeation properties through bacterial porins. *Biochemistry 49*, 6928−6935.
(57) Hajjar, E., Mahendran, K. R., Kumar, A., Bessonov, A., Petrescu, M., Weingart, H., Ruggerone, P., Winterhalter, M., and Ceccarelli, M. (2010) Bridging timescales and length scales: From macroscopic flux to the molecular mechanism of antibiotic diffusion through porins. *Biophys. J. 98*, 569−575.
(58) Kumar, A., Hajjar, E., Ruggerone, P., and Ceccarelli, M. (2010) Molecular simulations reveal the mechanism and the determinants for ampicillin translocation through OmpF. *J. Phys. Chem. B 114*, 9608−9616.
(59) Smart, O. S., Neduvelil, J. G., Wang, X., Wallace, B. A., and Sansom, M. S. (1996) HOLE: A program for the analysis of the pore dimensions of ion channel structural models. *J. Mol. Graphics 14*, 354−360 , 376.
(60) Pettersen, E. F., Goddard, T. D., Huang, C. C., Couch, G. S., Greenblatt, D. M., Meng, E. C., and Ferrin, T. E. (2004) UCSF Chimera: A visualization system for exploratory research and analysis. *J. Comput. Chem. 25*, 1605−1612.